THE JOURNAL OF BIOLOGICAL CHEMISTRY VOL. 290, NO. 23, pp. 14278–14288, June 5, 2015

Thioredoxin Selectivity for Thiol-based Redox Regulation of Target Proteins in Chloroplasts*

Received for publication, February 23, 2015, and in revised form, April 14, 2015 Published, JBC Papers in Press, April 15, 2015, DOI 10.1074/jbc.M115.647545

Keisuke Yoshida[‡§], **Satoshi Hara**[‡], **and Toru Hisabori**[‡§1]

From the [‡]*Chemical Resources Laboratory, Tokyo Institute of Technology, Nagatsuta 4259-R1-8, Midori-ku, Yokohama 226-8503, and* [§]*Core Research for Evolutional Science and Technology (CREST), Japan Science and Technology Agency (JST), Tokyo 102-0075, Japan*

Background: Thioredoxin (Trx) plays a pivotal role in the redox regulation of target proteins.
Results: Functional diversity of chloroplast Trxs was determined by observing Trx-dependent redox shifts of several thiol-modulated enzymes *in vitro* and *in vivo*.
Conclusion: Novel insights into the chloroplast redox network were provided.
Significance: Our results shed light on the molecular basis of the light-responsive adjustment of chloroplast functions.

Redox regulation based on the thioredoxin (Trx) system is believed to ensure light-responsive control of various functions in chloroplasts. Five Trx subtypes have been reported to reside in chloroplasts, but their functional diversity in the redox regulation of Trx target proteins remains poorly clarified. To directly address this issue, we studied the Trx-dependent redox shifts of several chloroplast thiol-modulated enzymes *in vitro* and *in vivo*. *In vitro* assays using a series of *Arabidopsis* recombinant proteins provided new insights into Trx selectivity for the redox regulation as well as the underpinning for previous suggestions. Most notably, by combining the discrimination of thiol status with mass spectrometry and activity measurement, we identified an uncharacterized aspect of the reductive activation of NADP-malate dehydrogenase; two redox-active Cys pairs harbored in this enzyme were reduced via distinct utilization of Trxs even within a single polypeptide. In our *in vitro* assays, Trx-*f* was effective in reducing all thiol-modulated enzymes analyzed here. We then investigated the *in vivo* physiological relevance of these *in vitro* findings, using *Arabidopsis* wild-type and Trx-*f*-deficient plants. Photoreduction of fructose-1,6-bisphosphatase was partially impaired in Trx-*f*-deficient plants, but the global impact of Trx-*f* deficiency on the redox behaviors of thiol-modulated enzymes was not as striking as expected from the *in vitro* data. Our results provide support for the *in vivo* functionality of the Trx system and also highlight the complexity and plasticity of the chloroplast redox network.

Thioredoxin (Trx)[2] is a small ubiquitous protein that plays a crucial role in the thiol-based redox regulation of a specific set of biological systems. Trx has a conserved WCGPC motif at an active site, enabling a dithiol-disulfide exchange reaction with target proteins. In chloroplasts, Trx receives reducing equivalents from the light-driven photosynthetic electron transport chain through ferredoxin-Trx reductase. The reduced form of Trx subsequently transfers reducing equivalents to specific disulfide bonds on target proteins, allowing modulation of enzymatic activities. It has been well documented that this redox cascade ensures a light-responsive control of chloroplast functions (1).

Our understanding of chloroplast thiol-modulated enzymes has grown dramatically since the development of proteomics-based methodologies for determining Trx-interacting proteins in 2001 (2, 3). In addition to classically known light-activated enzymes such as Calvin cycle enzymes (*e.g.* fructose-1,6-bisphosphatase (FBPase) and sedoheptulose-1,7-bisphosphatase (SBPase)) and NADP-malate dehydrogenase (NADP-MDH) (1), a number of chloroplast proteins have been newly described as Trx target candidates to date (4–6). Some of them have been further investigated in detail by biochemical and/or reverse genetic studies, providing important indications that the chloroplast Trx system engages in crosstalk with a diverse array of chloroplast functions, including starch synthesis (7), tetrapyrrole metabolism (8, 9), and the antioxidant defense system (10–12).

The chloroplast Trx system in plants is also characterized by a large Trx family composed of Trx-*f*, -*m*, -*x*, -*y*, and -*z* (13). Trx-*f* and Trx-*m* were initially identified as effective activators of FBPase and NADP-MDH, respectively (14, 15). Trx-*x*, Trx-*y*, and Trx-*z* were discovered with the increased availability of plant genome information and reported to be efficient in donating reducing equivalents to antioxidant defense systems (10, 11, 16). Trx-*z* was also shown to act as a decisive regulator for plastidial transcription (17).

Given the localization of divergent Trx subtypes and Trx target proteins in chloroplasts, it is readily conceivable that chloroplasts host a complex redox network for elaborate regulation

* This work was supported in part by the Core Research of Evolutional Science and Technology program (CREST) from the Japan Science and Technology Agency (JST) and Grant-in-aid for Scientific Research 26840090 (to K. Y.) from the Japan Society for the Promotion of Science.
[1] To whom correspondence should be addressed: Chemical Resources Laboratory, Tokyo Institute of Technology, Nagatsuta 4259-R1-8, Midori-Ku, Yokohama 226-8503, Japan. Tel.: 81-45-924-5234; Fax: 81-45-924-5268; E-mail: thisabor@res.titech.ac.jp.
[2] The abbreviations used are: Trx, thioredoxin; FBPase, fructose-1,6-bisphosphatase; SBPase, sedoheptulose-1,7-bisphosphatase; NADP-MDH, NADP-malate dehydrogenase; PrxQ, peroxiredoxin-Q; AMS, 4-acetamido-4′-maleimidylstilbene-2,2′-disulfonate; CBB, Coomassie Brilliant Blue R-250; DNA-Mal, DNA-maleimide.

of many chloroplast functions. Although functional specificity and redundancy of different Trx subtypes have been partly reported as mentioned above, little consistent description has been achieved. For example, Trx-*m* was originally defined as the most favorable partner for NADP-MDH activation (14, 15), but it was later shown that Trx-*f* can also activate NADP-MDH with an efficiency comparable with or even higher than that of Trx-*m* (10, 18, 19). Such ambiguity may reflect the reality that almost all hypotheses in this field have been based solely on the monitoring of enzymatic activity, and not on the direct observation of the redox state. Furthermore, very few attempts have been made to clarify *in vivo* Trx selectivity for the redox regulation of target proteins. Consequently, there seems to be a critical gap in the current knowledge of the chloroplast redox network.

To fill this gap, direct observation of Trx-dependent reduction of chloroplast thiol-modulated enzymes is desirable in both biochemical and physiological contexts. In this study, we have clarified some novel aspects of the functional diversity of Trxs and of *in vivo* redox dynamics in chloroplasts, providing an important step toward advancing the understanding of the chloroplast redox network and of plant strategies for adapting to fluctuating light environments.

Experimental Procedures

Preparation of Expression Plasmids—Total RNA was isolated from *Arabidopsis thaliana* as described previously (20) and used as a template for RT-PCR. Gene fragments encoding the mature protein region (predicted by TargetP) of Trx-*f*1 (At3g02730), Trx-*f*2 (At5g16400), Trx-*m*2 (At4g03520), Trx-*m*4 (At3g15360), Trx-*x* (At1g50320), Trx-*y*1 (At1g76760), Trx-*z* (At3g06730), FBPase (At3g54050), SBPase (At3g55800), NADP-MDH (At5g58330), and peroxiredoxin-Q (PrxQ; At3g26060) were cloned into the pET-23a (for Trx-*f*2, Trx-*m*2, Trx-*x*, Trx-*y*1, FBPase, and PrxQ) or pET-23c (for Trx-*f*1, Trx-*m*4, Trx-*z*, SBPase, and NADP-MDH) expression vector (Novagen). The Trx-*f*2 plasmid was designed to express His-tagged protein at the C terminus because of the technical limit of the purification (see below).

Protein Expression and Purification—Each expression plasmid was transformed into *Escherichia coli* strain BL21 (DE3). The transformed cells were cultured at 37 °C. Expression was induced by the addition of 0.5 mM isopropyl-1-thio-β-D-galactopyranoside followed by further culture at 21 °C overnight. The cells were disrupted by sonication. After centrifugation (125,000 × *g* for 40 min), the resulting supernatant was used to purify the protein of interest. Each protein except for Trx-*f*2 was purified by a combination of anion exchange chromatography, using a DEAE-Toyopearl 650M column (Tosoh) and Q-Toyopearl 600C column (Tosoh), and hydrophobic interaction chromatography, using a butyl-Toyopearl 650M column (Tosoh). Purification was performed in a medium containing 25 mM Tris-HCl (pH 7.5–8.1), 1 mM EDTA, and 0.5 mM DTT, but EDTA and DTT were removed by dialysis after purification. The His-tagged Trx-*f*2 was purified as described previously (21). All the purification procedures were performed at 4 °C. Trx-*h*1 and Trx-*o*1 proteins were prepared in our previous studies (22, 23). Protein concentration was determined with a BCA protein assay (Pierce).

Insulin Reduction Assay of Trxs—The dithiol-disulfide exchange ability of Trxs was measured as the change in turbidity of an insulin solution due to the precipitation of the free insulin B chain by reduction (24). The assay mixture contained 50 mM Tris-HCl (pH 7.5), 50 mM NaCl, 1 mM EDTA, 230 μM bovine insulin, and 0.5 mM DTT. Change in turbidity was monitored at 650 nm at 25 °C.

Determination of the Midpoint Redox Potential of Trxs—The midpoint redox potential (E_m) of Trxs was determined as described previously (25) with modifications. Each recombinant Trx (0.6 μM) was incubated in 25 mM Tris-HCl (pH 7.5), 50 mM oxidized DTT, and various concentrations of reduced DTT (0.001–50 mM). After incubation for 3 h at 25 °C, Trx was precipitated with 10% (v/v) TCA and washed with ice-cold acetone. Precipitants were then suspended by SDS sample buffer (62.5 mM Tris-HCl (pH 6.8), 2% (w/v) SDS, 7.5% (v/v) glycerol, and 0.01% (w/v) bromphenol blue) containing the thiol-modifying reagent 4-acetamido-4′-maleimidylstilbene-2,2′-disulfonate (AMS). After labeling for 1 h at room temperature, protein samples were subjected to nonreducing SDS-PAGE. Proteins were stained with Coomassie Brilliant Blue R-250 (CBB). The E_m value of Trxs was calculated by fitting the titration data of the reduction level of Trxs to the Nernst equation. A value of −357 mV was used as the E_m of DTT at pH 7.5, which was given by the observation that the E_m of DTT is −327 mV at pH 7.0 and shows the linear pH dependence of −59 mV/pH (26, 27).

Determination of the Redox State of Thiol-modulated Enzymes in Vitro—FBPase, SBPase, and NADP-MDH proteins were prepared in almost completely oxidized form, whereas approximately half of PrxQ was present in reduced form. PrxQ was accordingly completely oxidized with 0.1 mM H_2O_2 before the reduction assay. H_2O_2 was removed by dialysis after the oxidation treatment.

FBPase, SBPase, or NADP-MDH (2 μM each) was incubated with 1 μM Trx in a medium containing 50 mM Tris-HCl (pH 7.5), 50 mM NaCl, and 0.5 mM DTT. PrxQ (2 μM) was incubated with 0.1 or 1 μM Trx in a medium containing 50 mM Tris-HCl (pH 7.5), 50 mM NaCl, and several concentrations of DTT (0–500 μM). After incubation for 30 min at 25 °C, proteins were TCA-precipitated, labeled with AMS, and subjected to nonreducing SDS-PAGE as described earlier. Labeling of free thiols using DNA-maleimide (DNA-Mal) was performed as described previously (28).

Peptide Mapping Analysis—After separation on nonreducing SDS-PAGE, CBB-stained protein bands were excised from the gel and fully destained with 50 mM NH_4HCO_3 and 50% (v/v) acetonitrile. The gel slice was dried completely and then incubated with 50 mM NH_4HCO_3 containing 20 ng/μl trypsin at 37 °C overnight. Tryptic peptides were extracted from the gel with 0.1% (v/v) TFA with 50% (v/v) and 75% (v/v) acetonitrile, continuously. Whole extracts were concentrated with a centrifugal concentrator and desalted using $ZipTip_{C18}$ (Millipore). The peptide sample was spotted onto the matrix (α-cyano-4-hydroxycinnamic acid) and air-dried on a MALDI plate (MTP 384 target plate ground steel BC, Bruker Daltonics). MALDI mass spectra

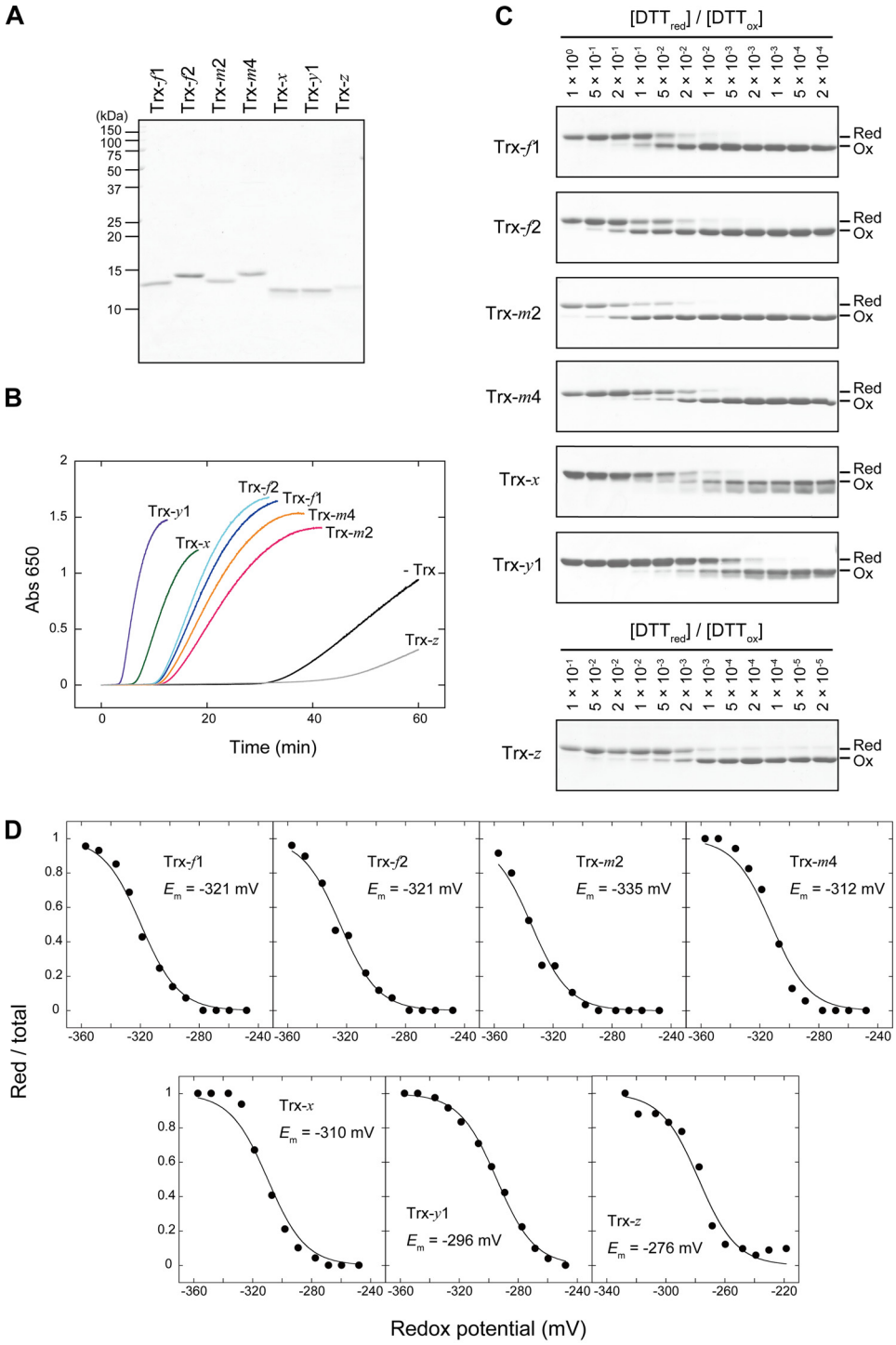

FIGURE 1. **Characteristics of recombinant Trxs in *Arabidopsis* chloroplasts.** *A*, SDS-PAGE profiles of purified recombinant Trxs. Only Trx-*f*2 was prepared as the His-tagged protein, which resulted in higher M_r (13,817.0) than that of Trx-*f*1 (13,119.2). *B*, monitoring of insulin reduction activity of Trxs. Time course of absorbance change at 650 nm (*Abs 650*) is shown. *C* and *D*, determination of the E_m of Trxs. *C*, Trxs were equilibrated with various (reduced DTT (*DTT$_{red}$*))/(oxidized DTT (*DTT$_{ox}$*)) ratios of redox buffers. Proteins were TCA-precipitated, labeled with AMS, loaded on nonreducing SDS-PAGE, and stained with CBB. *Red*, reduced form; *Ox*, oxidized form. *D*, the reduction level quantified as the ratio of the reduced form to the total was plotted against the redox potential of DTT buffer. The data were fitted to the Nernst equation, and each E_m value was determined. The E_m values are the mean of two independent titrations with deviations of <3 mV.

were obtained using an ultrafleXtreme-TK2 spectrometer (Bruker Daltonics). Results were queried with the Mascot search engine from Matrix Science to identify matched peptides.

Activity Measurement of NADP-MDH—After incubation with Trx as described earlier, NADP-MDH activity was monitored as a decrease in absorbance at 340 nm due to NADPH oxidation. The molar extinction coefficient for NADPH of 6200 M^{-1} cm^{-1} was used for calculation of the amounts of oxidized NADPH. Assays were performed in a medium containing 50 mM Tris-HCl (pH 7.5), 50 mM NaCl, indicated concentrations of oxaloacetic acid, indicated concentrations of NADPH, and 10 nM NADP-MDH at 25 °C.

Plant Materials—*A. thaliana* wild-type plant (Col-0) and T-DNA insertion mutants into *Trx-f1* (At3g02730) or *Trx-f2* (At5g16400) genes (*trxf1-1*; Salk_049146C, *trxf1-2*; Salk_099762C, *trxf1-3*; and Salk_128365C, *trxf2*; GK-020E05) were used in this study. Each homozygous mutant was backcrossed to the wild type and isolated again from the F_2 generation. The *trxf1 trxf2* double mutants (*trxf1-1 trxf2*, *trxf1-2 trxf2*, and *trxf1-3 trxf2*) were obtained by crossing each single mutant and screening from the F_2 generation. Screening was performed by genomic PCR using T-DNA-specific primer and *Trx-f1-* or *Trx-f2*-specific primers. Plants were grown in soil in a controlled growth chamber (70 μmol photons m^{-2} s^{-1}, 22 °C, relative humidity; 60%, 16 h/8 h day/night) for 4 weeks.

RT-PCR Analysis—Total RNA was isolated from *Arabidopsis* wild-type and *trxf* mutant plants as described earlier and used as a template for RT-PCR. RT-PCR was performed using ReverTra Ace (Toyobo) as the reverse transcriptase and KOD-Plus (Toyobo) as the DNA polymerase according to the manufacturer's instructions. The following primers were used: 5′-GAGACCTCACACACACTCTC-3′ and 5′-AACTGGAAACCTAAAGATAATC-3′ for *Trx-f1*, 5′-TTGGAAATCAAAAGTCTCCC-3′ and 5′-TGAACTTGTGATGCATACAG-3′ for *Trx-f2*, and 5′-CTGCCAGTAGTCATATGCTT-3′ and 5′-ACTACGGTTATCCGAGTAGT-3′ for *18s rRNA*.

Light-dependent Redox Behaviors of Trxs and Thiol-modulated Enzymes in Vivo—Plants were placed at the indicated light intensities (0–660 μmol photons m^{-2} s^{-1}) for 15 min at 25 °C and used for the determination of the *in vivo* reduction level of Trxs and thiol-modulated enzymes as described previously (21). Antibodies against Trx-*f*1, Trx-*m*4, Trx-*x*, Trx-*y*1, Trx-*z*, and SBPase were newly prepared using each recombinant protein as the antigen. For PrxQ immunodetection, a commercially available polyclonal antibody (Agrisera) was used.

Results

Trx Selectivity for Redox Regulation of FBPase, SBPase, and PrxQ in Vitro—In *Arabidopsis*, Trx-*f*, Trx-*m*, Trx-*x*, Trx-*y*, and Trx-*z* are encoded by two, four, one, two, and one nuclear genes, respectively (13). Isoforms of each Trx subtype generally show high homology of amino acid sequence in the mature protein region (*e.g.* Trx-*f*1 and Trx-*f*2, 88%; Trx-*m*1 and Trx-*m*2, 81%), suggesting that they have similar properties. Then we transformed some of these genes into *E. coli* and prepared recombinant proteins for five Trx subtypes as shown in Fig. 1*A*. Except for Trx-*z*, they were confirmed by the insulin reduction assay to be capable of dithiol-disulfide exchange reaction (Fig. 1*B*). Redox titration of Trxs with reduced and oxidized DTT indicated that E_m of Trx-*z* is less negative than that of other Trxs (Fig. 1, *C* and *D*), which may relate to the lack of insulin reduction activity in Trx-*z*. However, Trx-*z* possessed an ability of the dithiol-disulfide exchange reaction, as a specific protein was reduced depending on this Trx (see below). Recombinant proteins of *Arabidopsis* chloroplast thiol-modulated enzymes including FBPase, SBPase, NADP-MDH, and PrxQ were also prepared. These recombinant proteins were used for comparing the efficiency of Trxs in reducing each thiol-modulated enzyme *in vitro*.

To gain clues for performing this experiment under near-physiological conditions, we roughly estimated the *in vivo* stoichiometry of Trxs to thiol-modulated enzymes. Using a dilution series of recombinant proteins and *Arabidopsis* leaf extracts, we successfully determined the *in vivo* amounts of some proteins (Fig. 2, *A* and *B*). Amounts of Trxs were almost within the same order of magnitude as those of thiol-modulated enzymes, although they varied depending on the protein species. Note that the *in vivo* amounts of some Trx isoforms were possibly overestimated because of cross-reaction with other isoforms (*e.g.* the Trx-*f*1 antibody also reacted with Trx-*f*2 with lower affinity; Fig. 2*C*). On the basis of these preliminary tests, we evaluated the *in vitro* Trx selectivity for redox regulation, under conditions where the molar ratio of Trx to thiol-modulated enzyme was 1:2 (μM) unless specified.

The redox state of thiol-modulated enzymes was determined by discriminating thiol status with the use of the thiol-modifying reagent AMS (see "Experimental Procedures"). As shown in Fig. 3*A*, only Trx-*f* assisted in the shift of FBPase from the oxidized to reduced forms. In contrast, Trx-*f* and Trx-*m* showed the capacity to reduce SBPase, but Trx-*f* showed higher efficiency (Fig. 3*B*). PrxQ plays a role in the detoxification of reactive oxygen species and is accordingly known as a component of the antioxidant system in chloroplasts (29). To fill this role, PrxQ must receive reducing equivalents from Trx (or other sources). The ability of each Trx for PrxQ reduction was evaluated with varying concentrations of Trx (0.1 or 1 μM) and DTT (0–500 μM) because it was anticipated that PrxQ is reduced by 0.5 mM DTT even in the absence of Trx (2). When each Trx was incubated at 0.1 μM with PrxQ, only Trx-*y* apparently promoted PrxQ reduction (Fig. 4). When incubated at 1 μM, all Trxs promoted PrxQ reduction with different efficiencies; Trx-*x*, Trx-*y*, and Trx-*z* converted PrxQ to the reduced form even under lower (5–10 μM) concentrations of DTT. This result also confirmed the Trx-*z* capability for the dithiol-disulfide exchange reaction, although Trx-*z* did not show insulin reduction activity (Fig. 1*B*).

Two-step Reductive Activation Mechanism of NADP-MDH—NADP-MDH plays a key role in the export of excess reducing equivalents from chloroplasts (30). As shown in Fig. 5*A*, NADP-MDH adopted three distinct redox states, depending on the type of Trx co-incubated. This finding may reflect that two redox-active Cys pairs, Cys^{77}–Cys^{82} and Cys^{418}–Cys^{430} (*Arabidopsis* numbering), are conserved in the N- and C-terminal extensions of NADP-MDH, respectively (31). NADP-MDH showed the largest AMS-derived shift of molecular weight (M_r) when incubated with Trx-*f*. In contrast, Trx-*m* caused only a partial M_r shift of NADP-MDH. These results suggest that Trx-*f* can reduce both of the disulfide bonds, whereas Trx-*m* can reduce either the N-terminal or the C-terminal disulfide bond alone. Trx-*x*, Trx-*y*, or Trx-*z* did not cause the M_r shift of NADP-MDH, indicating that these Trxs can reduce neither N-terminal nor C-terminal disulfide bonds.

One disadvantageous point for AMS-based discrimination of thiol status is that, because of the small molecular mass of AMS (536.44 Da), it is difficult to determine the precise number of thiol groups involved in the redox regulation. To overcome this problem, we recently developed a new thiol-labeling reagent

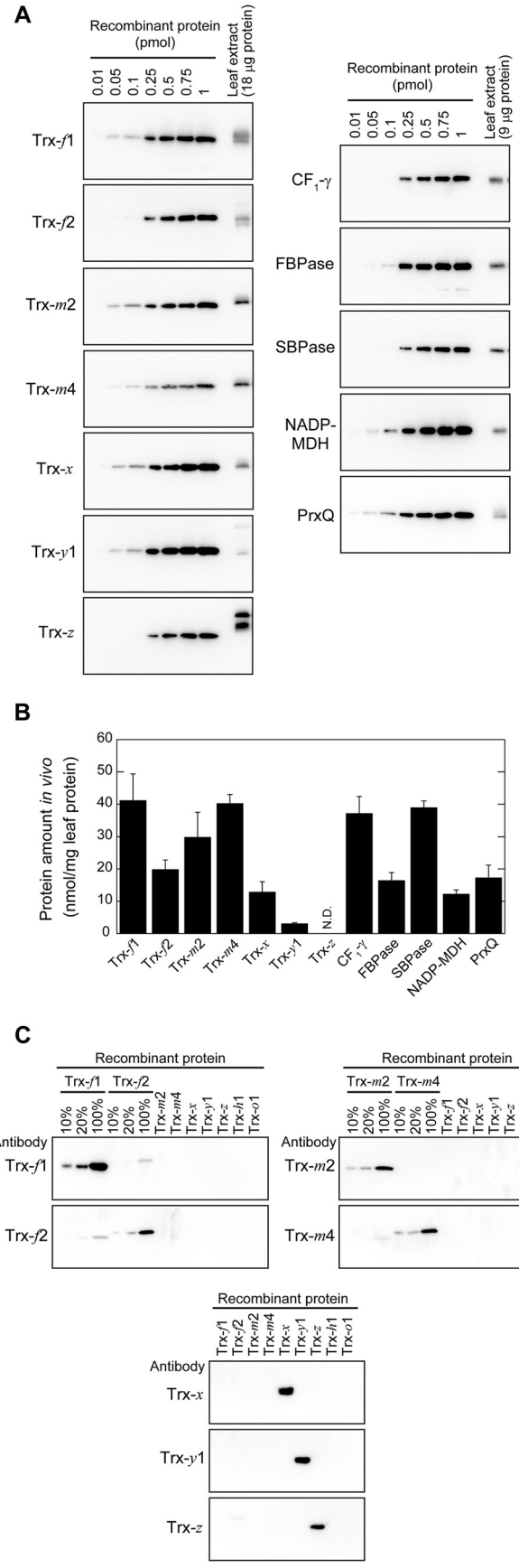

FIGURE 2. **Estimation of *in vivo* amounts of Trxs and thiol-modulated enzymes in *Arabidopsis* chloroplasts.** *A*, recombinant proteins and *Arabidopsis* leaf extracts were loaded on SDS-PAGE in the indicated protein amounts and then detected by immunoblotting analysis. *B*, *in vivo* amount of each protein was estimated using the regression of signal intensity on a dilution series of the recombinant proteins. Each value represents the mean ± S.D. (three different plants). *N.D.*, not determined. *C*, specificity of Trx antibodies. Recombinant Trxs were loaded on SDS-PAGE at 10 ng (100%) and detected by immunoblotting analysis.

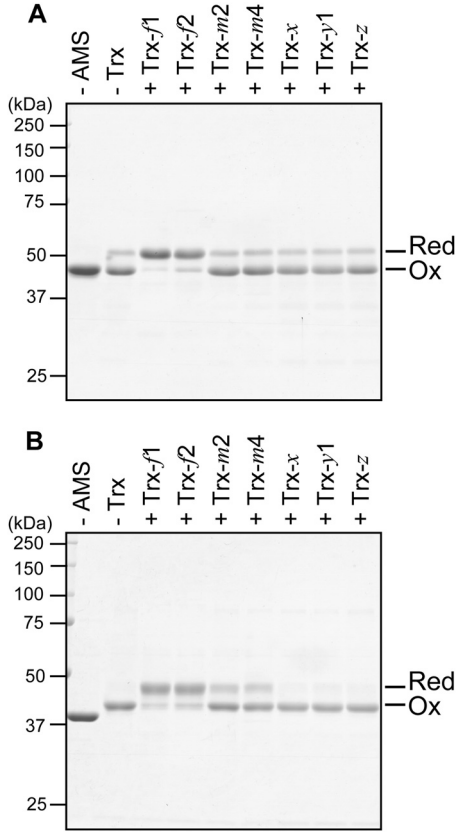

FIGURE 3. **Trx selectivity for the reduction of FBPase and SBPase.** *A* and *B*, 2 μM FBPase (*A*) or SBPase (*B*) was incubated with 1 μM Trx in the presence of 0.5 mM DTT. Proteins were TCA-precipitated, labeled with AMS, loaded on nonreducing SDS-PAGE, and stained with CBB. *Red*, reduced form; *Ox*, oxidized form. The difference in M_r between non-labeled (−*AMS*) and Ox form observed in SBPase (*B*) is due to the labeling of non redox-active free thiols.

DNA-Mal (28). DNA-Mal causes a larger change in SDS-PAGE mobility (~9 kDa per incorporated DNA-Mal molecule) of proteins and is, therefore, applicable for precise determination of the number of free thiols in the protein molecule. Using this reagent, we determined the number of free thiols that emerged in NADP-MDH by Trx-*f* and Trx-*m*, respectively. The molecular mass shifts caused by Trx-*f* and Trx-*m* were estimated to be 36.5 kDa (corresponding to four free thiols) and 18.7 kDa (two free thiols), respectively (Fig. 5*B*). These results strongly support the above mentioned hypothesis of distinct NADP-MDH-reducing abilities of Trx-*f* and Trx-*m*.

Our next question addressed the detailed mechanism of NADP-MDH reduction by Trx-*m*; of the two Cys pairs harbored in N- and C-terminal extensions, which one was reduced by Trx-*m*? To answer this question, the fully reduced, partially reduced, and oxidized forms of NADP-MDH shown in Fig. 5*A* were in-gel digested with trypsin, and mass spectra of the resulting peptides were compared (Fig. 6*A*). The theoretical M_r values of the tryptic peptides containing the N-terminal Cys

pair (Glu^{76} to Lys^{88}) and C-terminal Cys pair (Cys^{418} to Val^{443}) were 1553.8 and 2661.0, respectively (calculated using the ExPASy ProtParam tool). A specific peak of *m/z* 1551.7 was observed in the peptides prepared from the partially reduced and oxidized NADP-MDH, implying that this peak is associated with the peptide of Glu^{76} to Lys^{88} in which Cys^{77}–Cys^{82} forms the disulfide bond. Indeed, when a gel slice excised from the partially reduced form was fully reduced with DTT and then alkylated with iodoacetamide, the peak of *m/z* 1551.7 disappeared and a new peak of *m/z* 1667.7 emerged (Fig. 6*B*). This new peak corresponded to the M_r of Glu^{76} to Lys^{88} (containing carbamidomethyl Cys) in the Mascot search engine. These results clearly indicate that Trx-*m* efficiently reduces the C-terminal Cys pair (Cys^{418}–Cys^{430}) but not the N-terminal one (Cys^{77}–Cys^{82}).

We further investigated the Trx-dependent change in NADP-MDH activity (Fig. 6*C*). NADP-MDH showed the highest activity when incubated with Trx-*f*, whereas Trx-*m* could not fully activate NADP-MDH. NADP-MDH showed no activity in the absence of Trx or in the presence of Trx-*x*, Trx-*y*, or Trx-*z*. Taken together, we conclude that (i) NADP-MDH exerts maximal activity upon cleavage of both disulfide bonds at N- and C-terminal extensions by Trx-*f*, (ii) NADP-MDH is only partially activated upon cleavage of the C-terminal disulfide bond by Trx-*m*, and (iii) NADP-MDH is completely inactive when both of the Cys pairs form disulfide bonds.

In Vivo Redox Behaviors of Trxs and Thiol-modulated Enzymes in Chloroplasts in Arabidopsis Wild-type and Trx-f-deficient Plants—Our *in vitro* assays showed that Trx-*f* is widely used for the reduction of FBPase, SBPase, NADP-MDH, and PrxQ (Figs. 3–5). We finally asked whether these *in vitro* findings are functionally significant *in vivo*. For this purpose, *Arabidopsis* T-DNA insertion mutants in *Trx-f1* (*trxf1-1*, *trxf1-2*, and *trxf1-3*) and *Trx-f2* (*trxf2*) genes were prepared (Fig. 7*A*). The *trxf1 trxf2* double mutants were also generated by crossing each single mutant. RT-PCR analysis confirmed that *Trx-f1* and *Trx-f2* transcript levels are severely decreased or undetected in each corresponding mutant (Fig. 7*B*).

Wild-type and *trxf* mutant plants showed similar growth phenotypes (Fig. 7*A*). Immunoblotting analysis indicated that neither Trx-*f*1 nor Trx-*f*2 proteins were detected in *trxf1 trxf2* double mutants, whereas other Trxs were accumulated at the same level as in the wild-type plant (Fig. 7*C*). Despite the dele-

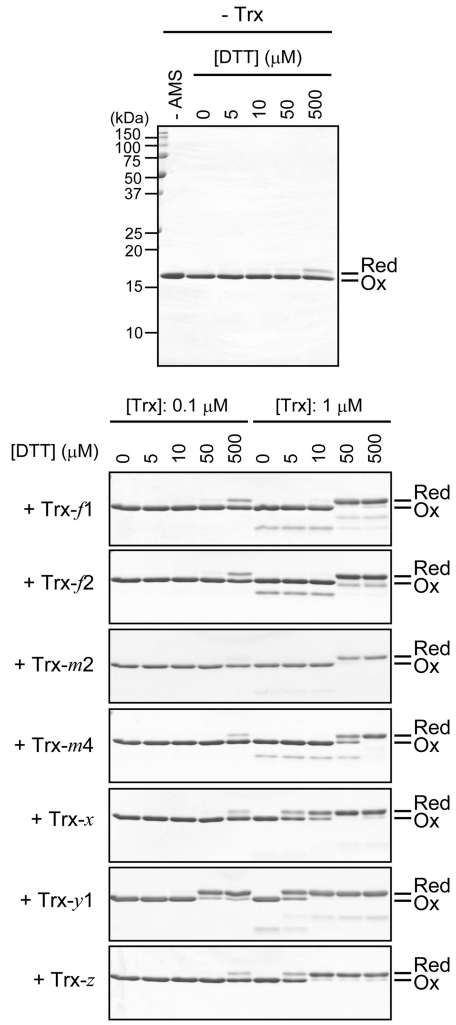

FIGURE 4. **Trx selectivity for the reduction of PrxQ.** Two μM PrxQ was incubated with 0.1 or 1 μM Trx in the presence of several concentrations of DTT (0–500 μM). Proteins were TCA-precipitated, labeled with AMS, loaded on nonreducing SDS-PAGE, and stained with CBB. Faint signals observed below the PrxQ band were derived from Trxs. *Red*, reduced form; *Ox*, oxidized form.

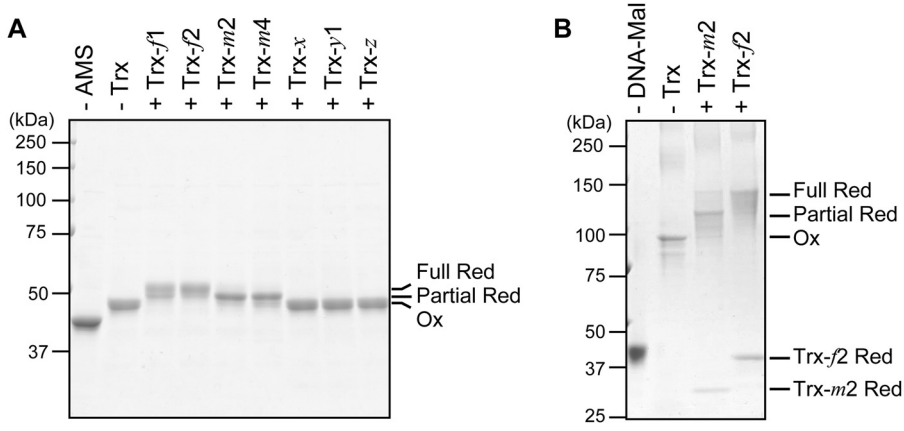

FIGURE 5. **Trx selectivity for the reduction of NADP-MDH.** *A* and *B*, 2 μM NADP-MDH was incubated with 1 μM Trx in the presence of 0.5 mM DTT. Proteins were TCA-precipitated, labeled with AMS (*A*) or DNA-Mal (*B*), loaded on nonreducing SDS-PAGE, and stained with CBB. *Full Red*, fully reduced form; *Partial Red*, partially reduced form; *Ox*, oxidized form. Differences in M_r between non-labeled (−*AMS*) (*A*) or non-labeled (−*DNA-Mal*) (*B*) and oxidized form are due to the labeling of non redox-active free thiols.

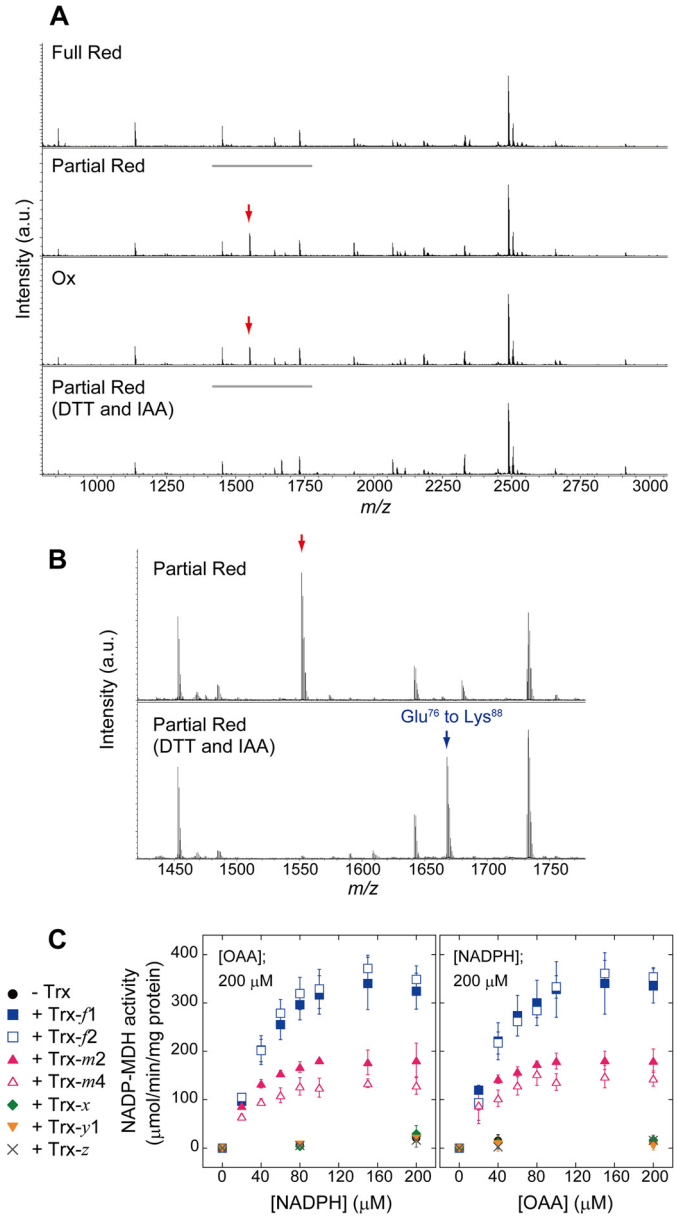

FIGURE 6. **Mechanism of two-step reductive activation of NADP-MDH.** *A* and *B*, peptide mapping analysis of NADP-MDH. Gel slices were excised from each redox state of NADP-MDH shown in Fig. 5*A*, and proteins were then in-gel digested with trypsin. For the partially reduced form, a gel slice was also treated with 10 mM DTT and then 55 mM iodoacetamide (*IAA*) before in-gel digestion. Peptide profiles were analyzed by mass spectrometry. The *m/z* range indicated by *gray bars* in *A* was expanded in *B*. The *red arrows* indicate a peak specifically observed in the peptides prepared from the partially reduced (*Partial Red*) and oxidized (*Ox*) forms. The *blue arrow* indicates a peak newly emerging following DTT and iodoacetamide treatments, corresponding to the Glu^{76} to Lys^{88} peptide (containing carbamidomethyl Cys) in the Mascot search engine. *Full Red*, fully reduced form. *C*, impacts of Trx on NADP-MDH activity. The saturation velocity curves for NADPH and oxaloacetic acid (*OAA*) are shown. Each value represents the mean ± S.D. ($n = 3$).

tion of *Trx-f2* transcript (Fig. 7*B*), Trx-*f*2 protein appears to be normally accumulated in the *trxf2* single mutant. This might be due to the cross-reaction of Trx-*f*2 antibody with Trx-*f*1 protein (Fig. 2*C*). This expectation is supported by the observation that Trx-*f*1 is the major form of Trx-*f* in *Arabidopsis* leaves (7).

Using these plants, we characterized the *in vivo* redox behaviors of Trxs and thiol-modulated enzymes in chloroplasts and evaluated the effects of Trx-*f* deficiency. In accordance with our previous data (21), Trx-*f* itself did not show a drastic redox shift upon illumination (Fig. 7*D*). In contrast, Trx-*m*, Trx-*x*, and Trx-*y* showed photoreduction responses, which were not uniform across the Trx family (Fig. 7, *E* and *F*). Chloroplast thiol-modulated enzymes including ATP synthase CF_1-γ subunit, FBPase, SBPase, and NADP-MDH also showed distinct light-responsive redox behaviors (Fig. 7, *E* and *F*). CF_1-γ was very efficiently reduced even under low light conditions. FBPase, SBPase, and NADP-MDH were shifted to the reduced form more gradually with increasing light intensity, although it was difficult to quantitatively evaluate the reduction level of NADP-MDH. The reduction level of PrxQ was maintained at a stable level (~70%) irrespective of light conditions.

Photoreduction of FBPase was partially impaired in *trxf1* and *trxf1 trxf2* mutants (Fig. 7, *E* and *F*). For example, the FBPase reduction level at 660 μmol photons m^{-2} s^{-1} in *trxf1 trxf2* mutants was 25% lower than that in the wild-type plant. It was thus evident that Trx-*f* is directly involved in the redox regulation of FBPase *in vivo*. However, it should be noted that more than half of FBPase could be reduced even in *trxf1 trxf2* mutants. Furthermore, other thiol-modulated enzymes examined here did not show a clear change in photoreduction patterns in *trxf* mutants. These unexpected consequences suggest the possibility that, together with the Trx system, other redox pathways cooperatively function in the chloroplast redox regulation in illuminated leaves.

Discussion

It is generally acknowledged that the chloroplast redox regulation system serves to transmit light signal from the photosynthetic electron transport chain to thiol-modulated enzymes and thereby ensures light-responsive control of a variety of chloroplast functions (1, 4–6). This scenario is certainly operative in plants, as shown by our recent study revealing the light-responsive redox dynamics of chloroplast thiol-modulated enzymes (21). It remains, however, to be uncovered how the underlying redox network is orchestrated in chloroplasts. To gain insights into this critical question, we addressed Trx selectivity for the redox regulation by directly observing Trx-dependent change in the redox state of target proteins.

It has been demonstrated by site-directed mutagenesis studies (32) and structural analyses (33) that FBPase forms a regulatory disulfide bond between Cys^{153} and Cys^{173} (or Cys^{178} upon mutation of Cys^{173}; pea numbering described in Refs. 32 and 33). Our results indicated that Trx-*f* plays a critical role in the cleavage of this disulfide bond, whereas any other Trxs fail to reduce it (Fig. 3*A*). These results agree strikingly with previous findings that only Trx-*f* can substantially enhance the enzymatic activity of FBPase (10, 14, 15, 19). In the case of SBPase, the redox-active Cys residues were identified (34), but the Trx selectivity responsible for the redox regulation has been little characterized. We have reported here that SBPase is reduced primarily by Trx-*f* and less efficiently by Trx-*m* (Fig. 3*B*). Similar trends of Trx efficiency were exemplified in the activation of glyceraldehyde-3-phosphate dehydrogenase and phosphoribulokinase (35). These results indicate that (i) Trx-*f* plays the predominant role in the reductive activation of Calvin cycle

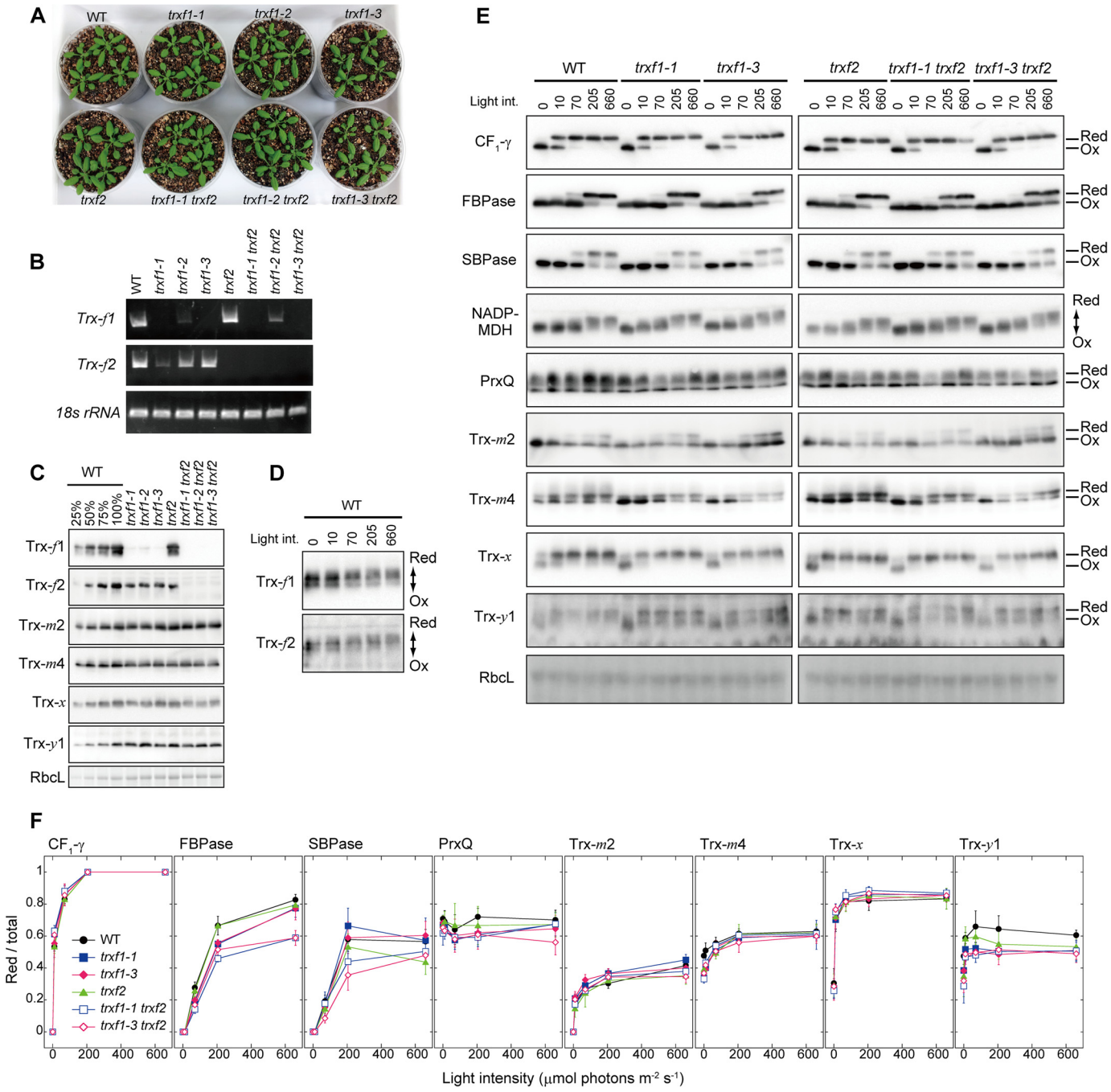

FIGURE 7. ***In vivo* redox behaviors of Trxs and thiol-modulated enzymes in chloroplasts in *Arabidopsis* WT and Trx-*f*-deficient plants.** *A*, growth phenotypes of *Arabidopsis* WT and *trxf* mutant plants. *B*, RT-PCR analysis. The transcript levels of *Trx-f* genes were examined. As a control, *18s rRNA* was also examined. *C*, immunoblotting analysis of chloroplast Trxs. The same amount of leaf total protein was loaded into each lane. As a loading control, Rubisco large subunit (*RbcL*) was stained with CBB. *D* and *E*, photoreduction of Trxs and thiol-modulated enzymes in chloroplasts. Experiments were performed under indicated light conditions (0–660 μmol photons m^{-2} s^{-1}). The same amount of leaf total protein was loaded into each lane. As a loading control, Rubisco large subunit (*RbcL*) was stained with Ponceau S. *Light int.*, light intensity. *Red*, reduced form; *Ox*, oxidized form. *F*, the reduction level of Trxs and thiol-modulated enzymes in chloroplasts. The reduction level was quantified as the ratio of the reduced form to the total. Each value represents the mean ± S.D. (three biological replicates).

enzymes, (ii) Trx-*m* is also involved to a lesser extent, and (iii) other Trxs are inefficient.

All types of Trx were capable of reducing PrxQ, but their efficiencies were not equivalent (Fig. 4). Trx-*y* was the most efficient reducer of PrxQ, followed by Trx-*x* and Trx-*z*. This result correlates with the study showing the distinct effects of Trxs on peroxidase activity of PrxQ (11). It has also been shown that Trx-*x* possesses high ability to reduce 2-Cys Prx (10, 11) and that Trx-*z* can act as an electron donor for several antioxidant enzymes (16). Notably, a recent study using several Trx mutants in *Arabidopsis* showed that the activity of methionine sulfoxide reductase was lowered in Trx-*y*-deficient plants, suggesting crosstalk between Trx-*y* and methionine sulfoxide reductase *in vivo* (12). These findings, together with our present

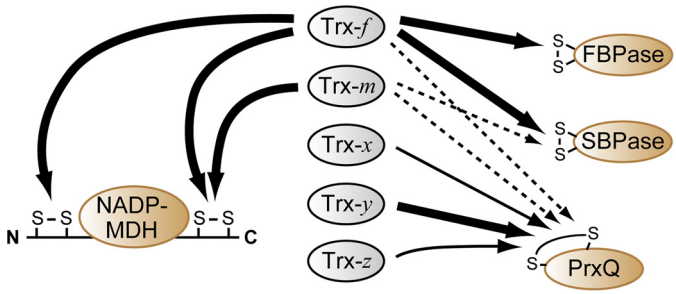

FIGURE 8. **A possible redox network between five Trxs and four Trx target proteins in chloroplasts suggested by the *in vitro* assay.** Trx efficiencies in the reduction of each protein are represented as the thickness of arrows: *solid bold arrows*, high; *solid thin arrows*, middle; and *dotted arrows*, low.

results, suggest that Trx-*x*, Trx-*y*, and Trx-*z* can be regarded as compatible partners in various antioxidant systems for supplying reducing equivalents.

The complex mechanism of NADP-MDH redox regulation has been well described based on accumulated biochemical and structural studies (36–43). Using the discrimination of thiol status combined with mass spectrometry and activity measurement, we further found that N- and C-terminal disulfide bonds harbored in NADP-MDH were reduced via distinct Trx selectivity even within a single polypeptide. Although Trx-*f* could fully activate NADP-MDH by cleaving both of two disulfide bonds, Trx-*m* allowed only partial activation due to the inability to cleave the N-terminal one (Figs. 5 and 6). Other Trxs could reduce neither N-terminal nor C-terminal disulfide bonds of NADP-MDH, keeping this enzyme completely inactive (Figs. 5 and 6). These findings coincide with the currently accepted model of NADP-MDH redox regulation: N-terminal disulfide bond formation is involved in a change in the whole NADP-MDH structure, whereas C-terminal disulfide bond formation results directly in blocking of the pathway for the substrate (31).

These results allow us to draw an outline of a redox network composed of five Trxs and four Trx target proteins in chloroplasts (Fig. 8). An important question is how the distinct efficiencies of Trxs in reducing each target protein are defined. The difference in E_m among Trxs does not seem to be the major determinant because there was little correspondence between this factor (Fig. 1, *C* and *D*) and Trx selectivity for redox regulation (Figs. 3–5). An alternative possible factor is the surface electrostatic potential on Trxs, Trx target proteins, and their interrelationships. Three-dimensional modeling of the Trx structure indicated that the proximal region to the active site of Trx-*f* is more positively charged than that of Trx-*m* (10, 44). Geck *et al.* (19) reported that the replacement of Lys (positively charged) located near the active site of Trx-*f* with Glu (negatively charged) drastically lowers the efficiency of FBPase activation. Involvement of surface electrostatic potential has also been implicated by studies using ATP synthase CF_1-γ subunit mutants; deletion or replacement of negatively charged residues close to the redox-active Cys pair in CF_1-γ strongly affects its property of Trx-dependent redox regulation (45–47). However, further studies are needed to gain deeper insights into the involvement of surface electrostatic potential in redox regulation. In this respect, structure determination of Trx and its target protein co-crystals will directly reveal the critical residues required for charge-charge interaction.

According to the model of redox pathways proposed on the basis of the *in vitro* data (Fig. 8), Trx-*f* is likely to play the predominant role in the redox regulation of FBPase, SBPase, and NADP-MDH. CF_1-γ was also reported to be favorably reduced by Trx-*f* (48). Are these scenarios physiologically relevant in plants? Characterization of the *in vivo* redox behaviors of chloroplast thiol-modulated enzymes indicated that FBPase photoreduction was partially impaired in *trxf1* (lacking the major isoform of Trx-*f*) and *trxf1 trxf2* mutants (Fig. 7, *E* and *F*). This result provides direct evidence that Trx-*f* mediates the transfer of reducing equivalents to FBPase *in vivo*. An unexpected but intriguing finding is that FBPase could still be reduced under conditions even where Trx-*f* was completely lacking. Furthermore, redox behaviors of other proteins that we investigated showed no clear changes in any *trxf* mutants. Thus, other pathways, not addressed in this study, for transferring reducing equivalents must participate together in the redox regulation in chloroplasts. In other words, a chloroplast redox network may extend beyond the ferredoxin-Trx reductase/Trx system described in current textbooks. The NADPH/NADPH-Trx reductase C system and/or glutathione/glutaredoxin system seem to be strong candidates. Some NADPH/NADPH-Trx reductase C target proteins in chloroplasts have been reported to date (49–51), but information about them is still limited. Glutaredoxin target proteins were also screened by a proteomics-based procedure (52), but most of them are still putative. More importantly, the *in vivo* working dynamics and biological significance of these systems remain to be elucidated. These potential systems may confer more flexible and sophisticated regulatory ways on chloroplasts. Our results are valuable in highlighting the complexity and plasticity of the chloroplast redox network and providing an important step toward its clarification.

Acknowledgments—We acknowledge the Biomaterial Analysis Center in Tokyo Institute of Technology for supporting DNA sequencing, and Material Analysis Suzukake-dai Center, Technical Department, Tokyo Institute of Technology, for mass spectrometry analysis.

References

1. Buchanan, B. B. (1980) Role of light in the regulation of chloroplast enzymes. *Annu. Rev. Plant Physiol.* **31,** 341–374
2. Motohashi, K., Kondoh, A., Stumpp, M. T., and Hisabori, T. (2001) Comprehensive survey of proteins targeted by chloroplast thioredoxin. *Proc. Natl. Acad. Sci. U.S.A.* **98,** 11224–11229
3. Yano, H., Wong, J. H., Lee, Y. M., Cho, M. J., and Buchanan, B. B. (2001) A strategy for the identification of proteins targeted by thioredoxin. *Proc. Natl. Acad. Sci. U.S.A.* **98,** 4794–4799
4. Hisabori, T., Motohashi, K., Hosoya-Matsuda, N., Ueoka-Nakanishi, H., and Romano, P. G. (2007) Towards a functional dissection of thioredoxin networks in plant cells. *Photochem. Photobiol.* **83,** 145–151
5. Montrichard, F., Alkhalfioui, F., Yano, H., Vensel, W. H., Hurkman, W. J., and Buchanan, B. B. (2009) Thioredoxin targets in plants: the first 30 years. *J. Proteomics* **72,** 452–474
6. Michelet, L., Zaffagnini, M., Morisse, S., Sparla, F., Pérez-Pérez, M. E., Francia, F., Danon, A., Marchand, C. H., Fermani, S., Trost, P., and Lemaire, S. D. (2013) Redox regulation of the Calvin-Benson cycle: something old, something new. *Front. Plant Sci.* **4,** 470
7. Thormählen, I., Ruber, J., von Roepenack-Lahaye, E., Ehrlich, S. M., Massot, V., Hümmer, C., Tezycka, J., Issakidis-Bourguet, E., and Geigenberger,

P. (2013) Inactivation of thioredoxin *f*1 leads to decreased light activation of ADP-glucose pyrophosphorylase and altered diurnal starch turnover in leaves of *Arabidopsis* plants. *Plant Cell Environ.* **36,** 16–29
8. Ikegami, A., Yoshimura, N., Motohashi, K., Takahashi, S., Romano, P. G., Hisabori, T., Takamiya, K., and Masuda, T. (2007) The CHLI1 subunit of *Arabidopsis thaliana* magnesium chelatase is a target protein of the chloroplast thioredoxin. *J. Biol. Chem.* **282,** 19282–19291
9. Luo, T., Fan, T., Liu, Y., Rothbart, M., Yu, J., Zhou, S., Grimm, B., and Luo, M. (2012) Thioredoxin redox regulates ATPase activity of magnesium chelatase CHLI subunit and modulates redox-mediated signaling in tetrapyrrole biosynthesis and homeostasis of reactive oxygen species in pea plants. *Plant Physiol.* **159,** 118–130
10. Collin, V., Issakidis-Bourguet, E., Marchand, C., Hirasawa, M., Lancelin, J. M., Knaff, D. B., and Miginiac-Maslow, M. (2003) The *Arabidopsis* plastidial thioredoxins: new functions and new insights into specificity. *J. Biol. Chem.* **278,** 23747–23752
11. Collin, V., Lamkemeyer, P., Miginiac-Maslow, M., Hirasawa, M., Knaff, D. B., Dietz, K. J., and Issakidis-Bourguet, E. (2004) Characterization of plastidial thioredoxins from *Arabidopsis* belonging to the new *y*-type. *Plant Physiol.* **136,** 4088–4095
12. Laugier, E., Tarrago, L., Courteille, A., Innocenti, G., Eymery, F., Rumeau, D., Issakidis-Bourguet, E., and Rey, P. (2013) Involvement of thioredoxin y2 in the preservation of leaf methionine sulfoxide reductase capacity and growth under high light. *Plant Cell Environ.* **36,** 670–682
13. Serrato, A. J., Fernández-Trijueque, J., Barajas-López, J. D., Chueca, A., and Sahrawy, M. (2013) Plastid thioredoxins: a "one-for-all" redox-signaling system in plants. *Front. Plant Sci.* **4,** 463
14. Wolosiuk, R. A., Crawford, N. A., Yee, B. C., and Buchanan, B. B. (1979) Isolation of three thioredoxins from spinach leaves. *J. Biol. Chem.* **254,** 1627–1632
15. Schürmann, P., Maeda, K., and Tsugita, A. (1981) Isomers in thioredoxins of spinach chloroplasts. *Eur. J. Biochem.* **116,** 37–45
16. Chibani, K., Tarrago, L., Schürmann, P., Jacquot, J. P., and Rouhier, N. (2011) Biochemical properties of poplar thioredoxin z. *FEBS Lett.* **585,** 1077–1081
17. Arsova, B., Hoja, U., Wimmelbacher, M., Greiner, E., Ustün, S., Melzer, M., Petersen, K., Lein, W., and Börnke, F. (2010) Plastidial thioredoxin *z* interacts with two fructokinase-like proteins in a thiol-dependent manner: evidence for an essential role in chloroplast development in *Arabidopsis* and *Nicotiana benthamiana*. *Plant Cell* **22,** 1498–1515
18. Hodges, M., Miginiac-Maslow, M., Decottignies, P., Jacquot, J. P., Stein, M., Lepiniec, L., Crétin, C., and Gadal, P. (1994) Purification and characterization of pea thioredoxin f expressed in *Escherichia coli*. *Plant Mol. Biol.* **26,** 225–234
19. Geck, M. K., Larimer, F. W., and Hartman, F. C. (1996) Identification of residues of spinach thioredoxin *f* that influence interactions with target enzymes. *J. Biol. Chem.* **271,** 24736–24740
20. Yoshida, K., and Noguchi, K. (2009) Differential gene expression profiles of the mitochondrial respiratory components in illuminated *Arabidopsis* leaves. *Plant Cell Physiol.* **50,** 1449–1462
21. Yoshida, K., Matsuoka, Y., Hara, S., Konno, H., and Hisabori, T. (2014) Distinct redox behaviors of chloroplast thiol enzymes and their relationships with photosynthetic electron transport in *Arabidopsis thaliana*. *Plant Cell Physiol.* **55,** 1415–1425
22. Hara, S., and Hisabori, T. (2013) Kinetic analysis of the interactions between plant thioredoxin and target proteins. *Front. Plant Sci.* **4,** 508
23. Yoshida, K., Noguchi, K., Motohashi, K., and Hisabori, T. (2013) Systematic exploration of thioredoxin target proteins in plant mitochondria. *Plant Cell Physiol.* **54,** 875–892
24. Holmgren, A. (1979) Thioredoxin catalyzes the reduction of insulin disulfides by dithiothreitol and dihydrolipoamide. *J. Biol. Chem.* **254,** 9627–9632
25. Motohashi, K., and Hisabori, T. (2006) HCF164 receives reducing equivalents from stromal thioredoxin across the thylakoid membrane and mediates reduction of target proteins in the thylakoid lumen. *J. Biol. Chem.* **281,** 35039–35047
26. Hirasawa, M., Ruelland, E., Schepens, I., Issakidis-Bourguet, E., Miginiac-Maslow, M., and Knaff, D. B. (2000) Oxidation-reduction properties of the regulatory disulfides of sorghum chloroplast nicotinamide adenine dinucleotide phosphate-malate dehydrogenase. *Biochemistry* **39,** 3344–3350
27. Hutchison, R. S., Groom, Q., and Ort, D. R. (2000) Differential effects of chilling-induced photooxidation on the redox regulation of photosynthetic enzymes. *Biochemistry* **39,** 6679–6688
28. Hara, S., Nojima, T., Seio, K., Yoshida, M., and Hisabori, T. (2013) DNA-maleimide: an improved maleimide compound for electrophoresis-based titration of reactive thiols in a specific protein. *Biochim. Biophys. Acta* **1830,** 3077–3081
29. Dietz, K. J., Jacob, S., Oelze, M. L., Laxa, M., Tognetti, V., de Miranda, S. M., Baier, M., and Finkemeier, I. (2006) The function of peroxiredoxins in plant organelle redox metabolism. *J. Exp. Bot.* **57,** 1697–1709
30. Scheibe, R. (2004) Malate valves to balance cellular energy supply. *Physiol. Plant* **120,** 21–26
31. Miginiac-Maslow, M., and Lancelin, J. M. (2002) Intrasteric inhibition in redox signalling: light activation of NADP-malate dehydrogenase. *Photosynth. Res.* **72,** 1–12
32. Jacquot, J. P., Lopez-Jaramillo, J., Miginiac-Maslow, M., Lemaire, S., Cherfils, J., Chueca, A., and Lopez-Gorge, J. (1997) Cysteine-153 is required for redox regulation of pea chloroplast fructose-1,6-bisphosphatase. *FEBS Lett.* **401,** 143–147
33. Chiadmi, M., Navaza, A., Miginiac-Maslow, M., Jacquot, J. P., and Cherfils, J. (1999) Redox signalling in the chloroplast: structure of oxidized pea fructose-1,6-bisphosphate phosphatase. *EMBO J.* **18,** 6809–6815
34. Dunford, R. P., Durrant, M. C., Catley, M. A., and Dyer, T. A. (1998) Location of the redox-active cysteines in chloroplast sedoheptulose-1,7-bisphosphatase indicates that its allosteric regulation is similar but not identical to that of fructose-1,6-bisphosphatase. *Photosynth. Res.* **58,** 221–230
35. Marri, L., Zaffagnini, M., Collin, V., Issakidis-Bourguet, E., Lemaire, S. D., Pupillo, P., Sparla, F., Miginiac-Maslow, M., and Trost, P. (2009) Prompt and easy activation by specific thioredoxins of Calvin cycle enzymes of *Arabidopsis thaliana* associated in the GAPDH/CP12/PRK supramolecular complex. *Mol. Plant* **2,** 259–269
36. Issakidis, E., Miginiac-Maslow, M., Decottignies, P., Jacquot, J. P., Crétin, C., and Gadal, P. (1992) Site-directed mutagenesis reveals the involvement of an additional thioredoxin-dependent regulatory site in the activation of recombinant sorghum leaf NADP-malate dehydrogenase. *J. Biol. Chem.* **267,** 21577–21583
37. Issakidis, E., Saarinen, M., Decottignies, P., Jacquot, J. P., Crétin, C., Gadal, P., and Miginiac-Maslow, M. (1994) Identification and characterization of the second regulatory disulfide bridge of recombinant sorghum leaf NADP-malate dehydrogenase. *J. Biol. Chem.* **269,** 3511–3517
38. Issakidis, E., Lemaire, M., Decottignies, P., Jacquot, J. P., and Miginiac-Maslow, M. (1996) Direct evidence for the different roles of the N- and C-terminal regulatory disulfides of sorghum leaf NADP-malate dehydrogenase in its activation by reduced thioredoxin. *FEBS Lett.* **392,** 121–124
39. Ruelland, E., Lemaire-Chamley, M., Le Maréchal, P., Issakidis-Bourguet, E., Djukic, N., and Miginiac-Maslow, M. (1997) An internal cysteine is involved in the thioredoxin-dependent activation of sorghum leaf NADP-malate dehydrogenase. *J. Biol. Chem.* **272,** 19851–19857
40. Ruelland, E., Johansson, K., Decottignies, P., Djukic, N., and Miginiac-Maslow, M. (1998) The autoinhibition of sorghum NADP malate dehydrogenase is mediated by a C-terminal negative charge. *J. Biol. Chem.* **273,** 33482–33488
41. Carr, P. D., Verger, D., Ashton, A. R., and Ollis, D. L. (1999) Chloroplast NADP-malate dehydrogenase: structural basis of light-dependent regulation of activity by thiol oxidation and reduction. *Structure* **7,** 461–475
42. Johansson, K., Ramaswamy, S., Saarinen, M., Lemaire-Chamley, M., Issakidis-Bourguet, E., Miginiac-Maslow, M., and Eklund, H. (1999) Structural basis for light activation of a chloroplast enzyme: the structure of sorghum NADP-malate dehydrogenase in its oxidized form. *Biochemistry* **38,** 4319–4326
43. Goyer, A., Decottignies, P., Issakidis-Bourguet, E., and Miginiac-Maslow, M. (2001) Sites of interaction of thioredoxin with sorghum NADP-malate dehydrogenase. *FEBS Lett.* **505,** 405–408
44. Michelet, L., Zaffagnini, M., Marchand, C., Collin, V., Decottignies, P., Tsan, P., Lancelin, J. M., Trost, P., Miginiac-Maslow, M., Noctor, G., and

Lemaire, S. D. (2005) Glutathionylation of chloroplast thioredoxin f is a redox signaling mechanism in plants. *Proc. Natl. Acad. Sci. U.S.A.* **102,** 16478–16483
45. Konno, H., Yodogawa, M., Stumpp, M. T., Kroth, P., Strotmann, H., Motohashi, K., Amano, T., and Hisabori, T. (2000) Inverse regulation of F_1-ATPase activity by a mutation at the regulatory region on the γ subunit of chloroplast ATP synthase. *Biochem. J.* **352,** 783–788
46. Ueoka-Nakanishi, H., Nakanishi, Y., Konno, H., Motohashi, K., Bald, D., and Hisabori, T. (2004) Inverse regulation of rotation of F_1-ATPase by the mutation at the regulatory region on the γ subunit of chloroplast ATP synthase. *J. Biol. Chem.* **279,** 16272–16277
47. Kohzuma, K., Dal Bosco, C., Meurer, J., and Kramer, D. M. (2013) Light- and metabolism-related regulation of the chloroplast ATP synthase has distinct mechanisms and functions. *J. Biol. Chem.* **288,** 13156–13163
48. Schwarz, O., Schürmann, P., and Strotmann, H. (1997) Kinetics and thioredoxin specificity of thiol modulation of the chloroplast H^+-ATPase. *J. Biol. Chem.* **272,** 16924–16927
49. Pérez-Ruiz, J. M., Spínola, M. C., Kirchsteiger, K., Moreno, J., Sahrawy, M., and Cejudo, F. J. (2006) Rice NTRC is a high-efficiency redox system for chloroplast protection against oxidative damage. *Plant Cell* **18,** 2356–2368
50. Michalska, J., Zauber, H., Buchanan, B. B., Cejudo, F. J., and Geigenberger, P. (2009) NTRC links built-in thioredoxin to light and sucrose in regulating starch synthesis in chloroplasts and amyloplasts. *Proc. Natl. Acad. Sci. U.S.A.* **106,** 9908–9913
51. Richter, A. S., Peter, E., Rothbart, M., Schlicke, H., Toivola, J., Rintamäki, E., and Grimm, B. (2013) Posttranslational influence of NADPH-dependent thioredoxin reductase C on enzymes in tetrapyrrole synthesis. *Plant Physiol.* **162,** 63–73
52. Rouhier, N., Villarejo, A., Srivastava, M., Gelhaye, E., Keech, O., Droux, M., Finkemeier, I., Samuelsson, G., Dietz, K. J., Jacquot, J. P., and Wingsle, G. (2005) Identification of plant glutaredoxin targets. *Antioxid. Redox Signal.* **7,** 919–929